

## UPDATED BIG BANG NUCLEOSYNTHESIS COMPARED WITH *WILKINSON MICROWAVE ANISOTROPY PROBE* OBSERVATIONS AND THE ABUNDANCE OF LIGHT ELEMENTS

ALAIN COC

Centre de Spectrométrie Nucléaire et de Spectrométrie de Masse, IN2P3-CNRS and Université Paris Sud, Bâtiment 104, F-91405 Orsay Campus, France

ELISABETH VANGIONI-FLAM

Institut d'Astrophysique de Paris, CNRS, 98 bis, Boulevard Arago, F-75014 Paris, France

PIERRE DESCOUVEMONT AND ABDERRAHIM ADAHCHOUR<sup>1</sup>

Physique Nucléaire Théorique et Physique Mathématique, CP229, Université Libre de Bruxelles, B-1050 Brussels, Belgium

AND

CARMEN ANGULO

Centre de Recherches du Cyclotron, Université Catholique de Louvain, Chemin du Cyclotron 2, B-1348 Louvain-La-Neuve, Belgium

Received 2003 July 23; accepted 2003 September 24

### ABSTRACT

We improve standard big bang nucleosynthesis (SBBN) calculations by taking into account new nuclear physics analyses (the 2003 work of Descouvemont and coworkers). Using a Monte Carlo technique, we calculate the abundances of light nuclei (D, <sup>3</sup>He, <sup>4</sup>He, and <sup>7</sup>Li) versus the baryon-to-photon ratio. The results concerning  $\Omega_b h^2$  are compared with relevant astrophysical and cosmological observations: the abundance determinations in primitive media and the results from cosmic microwave background (CMB) experiments, especially the *Wilkinson Microwave Anisotropy Probe* (*WMAP*) mission. Consistency between *WMAP*, SBBN results, and D/H data strengthens the deduced baryon density and has interesting consequences on cosmic chemical evolution. A significant discrepancy between the calculated <sup>7</sup>Li abundance deduced from *WMAP* and the Spite plateau is clearly revealed. To explain this discrepancy, three possibilities are invoked: systematic uncertainties on the Li abundance, surface alteration of Li in the course of stellar evolution, or poor knowledge of the reaction rates related to <sup>7</sup>Be destruction. In particular, the possible role of the up to now neglected <sup>7</sup>Be(*d, p*)<sup>2</sup>α and <sup>7</sup>Be(*d, α*)<sup>5</sup>Li reactions is considered. Another way to reconcile these results coming from different horizons consists of invoking new, speculative primordial physics that could modify the nucleosynthesis emerging from the big bang and perhaps the CMB physics itself. The impressive advances in CMB observations provide a strong motivation for more efforts in experimental nuclear physics and high-quality spectroscopy to keep SBBN in pace.

*Subject headings:* cosmological parameters — early universe — nuclear reactions, nucleosynthesis, abundances

*On-line material:* color figures

### 1. INTRODUCTION

There exist different ways to determine the baryonic density of the universe. The “traditional method” is standard big bang nucleosynthesis (SBBN), which is based on nuclear physics in the early universe. This calculation reproduces the primordial light-element (D, <sup>3</sup>He, <sup>4</sup>He, and <sup>7</sup>Li) abundances over an interval of 10 orders of magnitude. Recently, however, the study of the cosmic microwave background (CMB) anisotropies and the census of the Lyα forest at high redshift have provided new methods for obtaining  $\Omega_b h^2$ . In the case of the CMB, the baryonic parameter ( $\Omega_b h^2$ , where *h* is the Hubble parameter expressed in units of 100 km s<sup>-1</sup> Mpc<sup>-1</sup>) is extracted from the amplitudes of the acoustic peaks in the angular power spectrum of the anisotropies. The  $\Omega_b h^2$  values deduced from these three different methods are in rather good agreement but may not be totally model independent.

A series of data have been released by many experiments, but very recently, the *Wilkinson Microwave Anisotropy Probe* (*WMAP*) mission has delivered a wealth of results, based on the first year of observations (Spergel et al. 2003). The mean

value  $\Omega_b h^2 = 0.024 \pm 0.001$  agrees with the previous estimates, but the error bar is considerably reduced. When including constraints from other observations at complementary angular scales, the value  $\Omega_b h^2 = 0.0224 \pm 0.0009$  is obtained (Spergel et al. 2003), setting stringent constraints on the general discussion of the SBBN scenario.

In the case of the Lyα forest, the baryonic density is deduced from the study of the atomic H I and He II Lyα absorption lines observed on the line of sight to quasars (baryonic matter distributed on large scales, in the redshift range  $0 < z < 5$ ). Indeed, this evaluation, although indirect because of the relatively large ionization uncertainties, leads to results consistent with the two other methods ( $\Omega_b h^2 \sim 0.02$ ; Riediger et al. 1998). However, the baryonic density obtained in this way carries a relatively large error bar, which in the present context makes it less constraining.

Consequently, because of the large efforts made recently to determine the cosmological parameters, it is now mandatory to refine the SBBN analysis. In this paper, we update the study performed in Coc et al. (2002, hereafter CV02) in which we had exploited a set of reaction rates from the NACRE compilation (Angulo et al. 1999). We reconsider here the SBBN calculation using reaction rates obtained from a new analysis of the 10 most important nuclear reactions (Descouvemont

<sup>1</sup> Permanent address: Laboratoire de Physique des Hautes Energie et Astrophysique, FSSM, Université Caddi Ayyad, Marrakech, Morocco.

et al. 2003, hereafter DAA03). Moreover, we consider the impact on the SBBN results of these main reactions and, at the same time, study other reactions that could be potentially important for SBBN.

After a summary of the observational data concerning the light-isotope abundances and the new nuclear input, we use Monte Carlo calculations to obtain the abundances of light nuclei (D,  $^3\text{He}$ ,  $^4\text{He}$ , and  $^7\text{Li}$ ) versus the baryon-to-photon ratio, taking into account the uncertainties on nuclear reaction rates. We discuss both agreements and discrepancies in comparing calculations, abundance data, and *WMAP* results.

## 2. ABUNDANCES OF LIGHT ELEMENTS

The observation of the most primitive astrophysical sites in which abundances can be measured and their comparison with the SBBN calculations allow us to extract  $\Omega_b h^2$ . For a general discussion on the updated observational data, see the review of Olive (2003).

The primordial  $^4\text{He}$  abundance,  $Y_p$ , is derived from observations of metal-poor, extragalactic, ionized hydrogen (H II) regions.

We adopt here the two recent values of Izotov et al. (1999;  $Y_p = 0.2452 \pm 0.0015$ ) and Luridiana et al. (2003;  $Y_p = 0.2391 \pm 0.0020$ ), giving a relatively large range of abundance for this isotope. Indeed, when considering systematic uncertainties, Fields & Olive (1998) obtain the range  $Y_p = 0.238 \pm 0.002 \pm 0.005$ .

Deuterium is particularly fragile and is only destroyed in stellar processes. Hence, the primordial abundance should be represented, in principle, by the highest value observed in remote cosmological clouds on the line of sight of high-redshift quasars. This is what we adopted in CV02. However, recently, Kirkman et al. (2003) have obtained a new measurement of  $\text{D}/\text{H} = (2.42^{+0.35}_{-0.25}) \times 10^{-5}$ , and therefore,  $[\text{O}/\text{H}] = -2.79 \pm 0.05$ . They also give their best estimate of the primordial D abundance, namely,  $\text{D}/\text{H} = (2.78^{+0.44}_{-0.38}) \times 10^{-5}$ , averaging individual measurements toward five quasars, which we now adopt here. However, since the sample of cosmological clouds is very limited and the systematic errors of D/H values are difficult to estimate, this value has to be considered with caution. Indeed, Crighton et al. (2003) highlight important aspects of the analysis that were not explored in previous works, showing that the methods used in analyses of D/H in quasar spectra should be improved. For example, according to different hypotheses about contamination, they show that D/H in the absorber toward quasar PG 1718+4807 can be as high as  $4.2 \times 10^{-4}$  or significantly lower than  $3 \times 10^{-4}$ .

Since the discovery of the Spite plateau (Spite & Spite 1982), namely, the constant lithium abundance as a function of metallicity, many new observations have strengthened its existence. Ryan, Norris, & Beers (1999) and Ryan et al. (2000) have obtained a tight limit on the plateau abundance. Specifically, these authors take into account all possible contributions from extrapolation to zero metallicity,  $^7\text{Li}$  depletion mechanisms, and biases in the analysis. Their extrapolated value (at 95% confidence level) is  $\text{Li}/\text{H} = (1.23^{+0.68}_{-0.32}) \times 10^{-10}$ . Recently, Thévenin et al. (2001) have obtained Very Large Telescope UV-Visual Echelle Spectrograph high-resolution spectra of seven metal-poor stars in the globular cluster NGC 6397. Their mean value of lithium,  $A(\text{Li}) = 2.23 \pm 0.07$ , is consistent with the preceding one. Bonifacio et al. (2002), who have also observed this globular cluster, obtain a higher mean value:  $A(\text{Li}) = 2.34 \pm 0.056$ . The difference between these two evaluations lies in the

different effective temperatures adopted. Indeed, these two independent observations and analyses give an indication of the systematic errors involved in Li/H determination.

Both observers and experts on stellar atmospheres agree that the abundance determination in halo stars, and more particularly that of lithium, may require a sophisticated analysis. In this respect, the temperature scale is influential, and it is possible that the scale adopted by Ryan et al. (2000) underestimates the Li/H ratio. Moreover, the determination of Li/H in stars embedded in globular clusters is more questionable than in halo field stars, since globular cluster stars may be polluted by their environment. Therefore, it would be necessary to select in a first step, star by star, those that are less contaminated, i.e., the most adequate for giving a reliable Li/H abundance. Note, however, that stars from small globular clusters (such as NGC 6397) are representative of the halo stars (R. Cayrel 2003, private communication). In addition to the Ryan et al. (2000) range, adopted here as in CV02, we also consider, conservatively, the upper limit of the Bonifacio et al. (2002) value, namely,  $\text{Li}/\text{H} = 2.49 \times 10^{-10}$ . Note, however, that these globular cluster determinations, at  $[\text{Fe}/\text{H}] \approx -2$ , cannot be directly compared with the Ryan et al. (2000) extrapolated value.

$^3\text{He}$  has been measured recently by Bania, Rood, & Balser (2002) in H II regions, but because of the large scatter in the data and the complex Galactic history of this isotope, we cannot consider it as a good cosmological tracer (Vangioni-Flam et al. 2003).

## 3. SBBN WITH IMPROVED NUCLEAR INPUT

In our previous work (CV02), we performed Monte Carlo calculations to obtain statistical limits on the calculated abundances, mainly using the NACRE compilation of reaction rates (Angulo et al. 1999). One of the main innovative features of NACRE with respect to former compilations (Caughlan & Fowler 1988, hereafter CF88) is that uncertainties are analyzed in detail, and realistic lower and upper bounds for the rates are provided. However, since it is a general compilation for multiple applications, coping with a broad range of nuclear configurations, these bounds have not always been evaluated through a rigorous statistical methodology. Hence, in CV02, a simple uniform distribution between these bounds was assumed for the Monte Carlo calculations. Since this compilation was not specifically addressed to the nuclear reactions implied in the SBBN, it also had to be complemented by other sources (Smith, Kawano, & Malaney 1993; Brune et al. 1999). Two recent SBBN calculations have been made with updated reaction rates, one based on the Nollett & Burles (2000, hereafter NB00) compilation and another (Cyburt, Fields, & Olive 2001, hereafter CFO01) on a partial reanalysis of the NACRE compiled data. These works (NB00 and CFO01) have given better defined statistical limits to the reaction rates of interest for SBBN. One (NB00) has used spline functions to fit the astrophysical  $S$ -factors (see the definition in CV02), while the other (CFO01) has used the NACRE  $S$ -factors with a different normalization (restricted to SBBN energies.) In NACRE, data are in general fitted by either a Breit-Wigner formula (the shape of nuclear resonances) or a low-order polynomial for nonresonant contributions. Indeed, unlike in CFO01, the fits are not restricted to the energy range of SBBN, taking advantage of all data to constrain the nuclear factor. The use of low-order polynomials, or better theoretical  $S$ -factor shapes, rather than, e.g., splines, has the advantage of smoothing out the dispersion of

data arising from the measurement technique itself rather than from physics, when no sharp resonance is expected in the energy domain. Consequently, the CFO01 global normalization factors are different from those of NACRE. One should note, however, that the isotope yields obtained from SBBN calculations using the two compilations (NACRE and NB00) agree well, reinforcing the confidence in these analyses.

Nevertheless, in order to improve on the general NACRE compilation, DAA03 have reassessed carefully the main nuclear network (10 reactions) on the basis of an  $R$ -matrix analysis.  $R$ -matrix theory has been used for many decades in the nuclear physics community. It allows us to parameterize nuclear cross sections with a reduced set of parameters related to nuclear quantities such as resonance energies and partial widths. This method can be used for both resonant and nonresonant contributions to the cross section. (See DAA03 and references therein for details of the method.) The energy dependence of the fitted  $S$ -factors is now constrained by the Coulomb functions and  $R$ -matrix poles rather than by arbitrary polynomial or spline functions. Even though this method has been widely used in nuclear astrophysics (see, e.g., Barker & Kajino 1991 for a recent application to a nuclear astrophysics problem), this is the first time that it has been applied to SBBN reactions. In addition, this new compilation (DAA03) provides  $1\sigma$  statistical limits for each of the 10 rates:  ${}^2\text{H}(p, \gamma){}^3\text{He}$ ,  ${}^2\text{H}(d, n){}^3\text{He}$ ,  ${}^2\text{H}(d, p){}^3\text{H}$ ,  ${}^3\text{H}(d, n){}^4\text{He}$ ,  ${}^3\text{H}(\alpha, \gamma){}^7\text{Li}$ ,  ${}^3\text{He}(n, p){}^3\text{H}$ ,  ${}^3\text{He}(d, p){}^4\text{He}$ ,  ${}^3\text{He}(\alpha, \gamma){}^7\text{Be}$ ,  ${}^7\text{Li}(p, \alpha){}^4\text{He}$ , and  ${}^7\text{Be}(n, p){}^7\text{Li}$ . These rate limits are derived from the  $R$ -matrix parameter errors calculated during the fitting procedure (see DAA03). The two remaining reactions of importance,  $n \leftrightarrow p$  and  ${}^1\text{H}(n, \gamma){}^2\text{H}$  (Chen & Savage 1999) come from theory and are unchanged with respect to CV02.

We have redone our Monte Carlo calculations, this time using Gaussian distributions with parameters provided by the new compilation (DAA03) discussed above. We have calculated the mean and the variance of the  ${}^4\text{He}$ , D,  ${}^3\text{He}$ , and  ${}^7\text{Li}$  yields as a function of  $\eta$ , fully consistent with our previous analysis (CV02). The differences with CFO01 for the  ${}^7\text{Li}$  yield are probably due to their renormalization procedure of NACRE  $S$ -factors. Figure 1 displays the resulting abundance limits ( $1\sigma$ ; it was  $2\sigma$  in Fig. 4 of CV02) from SBBN calculations compared with primordial ones inferred from observations. It is important to note that the present results are in good agreement with CV02. With these improved calculations, we can now compare SBBN results, primitive abundances of the light elements, and baryonic density derived from CMB observations.

#### 4. DISCUSSION

Following numerous determinations of  $\Omega_b h^2$  through CMB observations, *WMAP* observations and subsequent analyses, including other observational constraints, have delivered a very precise value,  $\Omega_b h^2 = 0.0224 \pm 0.0009$ , corresponding to  $\eta = (6.14 \pm 0.25) \times 10^{-10}$  (Spergel et al. 2003). In their paper, this evaluation has been compared with the SBBN calculations of Burles, Nollett, & Turner (2001), leading to  $\text{D}/\text{H} = (2.62^{+0.18}_{-0.2}) \times 10^{-5}$ . With our improved analysis of SBBN reaction rates, using the *WMAP*  $\Omega_b h^2$  range together with these SBBN results (*WMAP*+SBBN hereafter), we can also deduce the primordial abundances as shown in Figure 1, in which is shown the *WMAP*  $\Omega_b h^2$  range intercepting the SBBN yield curves. The uncertainties on these abundances take into account the *WMAP*  $\Omega_b h^2$  uncertainty and the SBBN uncertainties

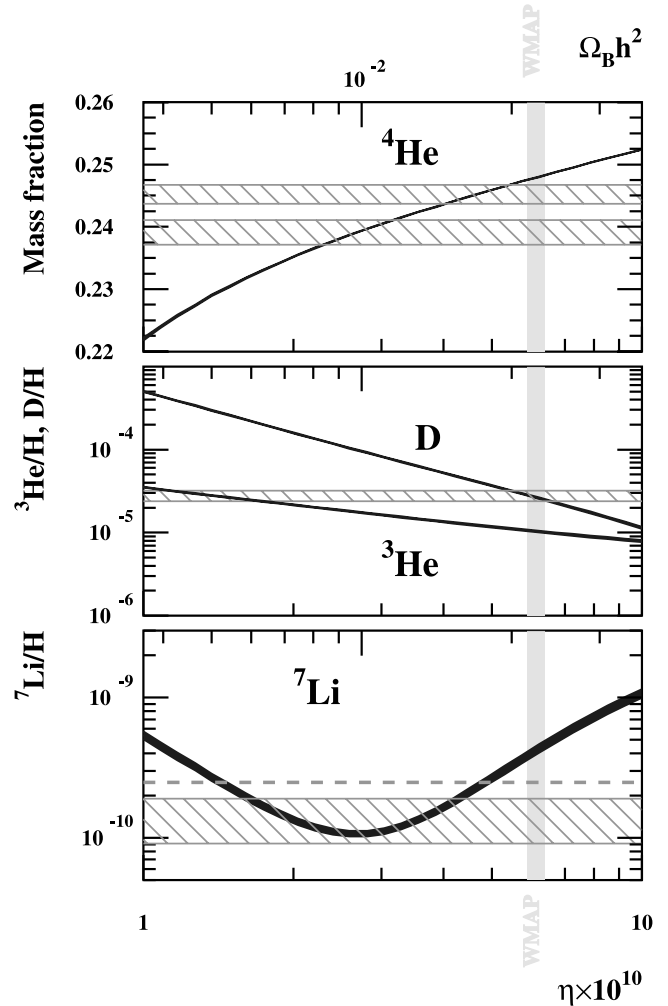


FIG. 1.—Abundances of  ${}^4\text{He}$  (mass fraction), D,  ${}^3\text{He}$ , and  ${}^7\text{Li}$  (by number relative to H) as a function of the baryon-to-photon ratio  $\eta$  or  $\Omega_b h^2$ . Limits ( $1\sigma$ ) are obtained from Monte Carlo calculations. The hatched regions represent primordial  ${}^4\text{He}$ , D, and  ${}^7\text{Li}$  abundances deduced from different primitive astrophysical sites (see § 2): Izotov et al. (1999; upper region) and Luridiana et al. (2003; lower region) for  ${}^4\text{He}$ , Kirkman et al. (2003) for D, and Ryan et al. (2000) for  ${}^7\text{Li}$  (95% confidence level). Concerning  ${}^7\text{Li}$ , we also show an upper limit derived from Bonifacio et al. (2002) observations (dashed line). The vertical stripe represents the ( $1\sigma$ )  $\Omega_b h^2$  limits provided by *WMAP* (Spergel et al. 2003). [See the electronic edition of the Journal for a color version of this figure.]

from DAA03 reaction rates. Our *WMAP*+SBBN deuterium primordial abundance is  $\text{D}/\text{H} = (2.60^{+0.19}_{-0.17}) \times 10^{-5}$ , which is in perfect agreement with the average value of  $(2.78^{+0.44}_{-0.38}) \times 10^{-5}$  (Kirkman et al. 2003) of  $\text{D}/\text{H}$  observations in cosmological clouds. The other primordial abundances deduced from *WMAP*+SBBN are  $Y_p = 0.2479 \pm 0.0004$  for the  ${}^4\text{He}$  mass fraction,  ${}^3\text{He}/\text{H} = (1.04 \pm 0.04) \times 10^{-5}$ , and  ${}^7\text{Li}/\text{H} = (4.15^{+0.49}_{-0.45}) \times 10^{-10}$ . Recently, Cyburt, Fields, & Olive (2003) have also compared SBBN and *WMAP* data. Their mean  $\text{D}/\text{H}$  value ( $2.75 \times 10^{-5}$ ) is slightly higher than our result, while  $Y_p$  is in good agreement. More importantly, their predicted  ${}^7\text{Li}$  ( $3.82 \times 10^{-10}$ ) is lower than our prediction (about 11%; see Table 1). The reason is probably the different normalization for nuclear data, as discussed above. It is timely to compare these primordial nucleosynthesis results with the observations described in § 2 and to explore the various astrophysical consequences.

TABLE 1  
SBBN RESULTS AT *WMAP*  $\Omega_b h^2$  FROM DIFFERENT AUTHORS

Source	$Y_p$	D/H ( $\times 10^{-5}$ )	$^3\text{He}/\text{H}$ ( $\times 10^{-5}$ )	Li/H ( $\times 10^{-10}$ )
This work.....	$0.2479 \pm 0.0004$	$2.60^{+0.19}_{-0.17}$	$1.04 \pm 0.04$	$4.15^{+0.49}_{-0.45}$
1.....	$0.2484^{+0.0004}_{-0.0005}$	$2.75^{+0.24}_{-0.19}$	$0.93^{+0.055}_{-0.054}$	$3.82^{+0.73}_{-0.60}$
2.....	...	$2.62^{+0.18}_{-0.22}$	...	...

REFERENCES.—(1) Cyburt et al. 2003; (2) Burles et al. 2001.

#### 4.1. Helium

As said previously, the  $^4\text{He}$  abundance determinations in H II regions are quite unsatisfactory because of observational uncertainties and the complex physics of H II regions. Luridiana et al. (2003) obtained a new determination of  $Y_p$  based on the abundance analysis of five metal-poor extragalactic H II regions. This relatively low value ( $0.2391 \pm 0.002$ ) differs significantly from the Isotov et al. (1999) higher value ( $0.2452 \pm 0.0015$ ) and the one deduced from *WMAP*+SBBN ( $0.2479$ ), but systematic uncertainties may prevail because of observational difficulties and complex physics (Fields & Olive 1998). In fact, the Isotov et al. (1999) interval (§ 2, Fig. 1) is only marginally compatible with the *WMAP* observations ( $\sim 8\%$  probability).

#### 4.2. Deuterium

*WMAP* observations together with our SBBN calculations lead to the mean primordial D/H value of  $2.60 \times 10^{-5}$ . In Figure 2 we plot D/H observations at high redshift (Burles & Tytler 1998; Tytler, Fan, & Burles 1996; O’Meara et al. 2001; D’Odorico, Dessauges-Zavadsky, & Molaro 2001; Pettini & Bowen 2001; Kirkman et al. 2003) that are thought to be representative of the D primordial abundances together with those inferred from SBBN calculations and the  $\Omega_b h^2$  range from *WMAP*. The stripe widths represent the uncertainty ( $1\sigma$ ) originating from both the *WMAP*  $\Omega_b h^2$  and nuclear uncertainties. It shows that this result is consistent with D/H observations at high redshift and specifically with the last measurement and averaged value of Kirkman et al. (2003). The convergence between these two independent methods seems to confirm this  $\Omega_b h^2$  evaluation. Adopting this result as a firm basis, one can draw some conclusions about the cosmic chemical evolution and the global star formation rate history in the universe. In addition to the high-redshift data, the only D/H observations available are (1) the protosolar value, which is affected by a large error bar, ( $2.5 \pm 0.5$ )  $\times 10^{-5}$  (Hersant, Gautier, & Huré 2001), and (2) the local and present value in the interstellar medium, ( $1.52 \pm 0.08$ )  $\times 10^{-5}$  (Moos et al. 2002). Accordingly, these observations can only set constraints on the chemical evolution of our Galaxy, showing that the star formation history is probably modest and smooth. It is worth noting that, in this context, D has barely been depleted between the big bang and the birth of the Sun, typically evolving from  $2.60 \times 10^{-5}$  to  $2.5 \times 10^{-5}$  during about 10 Gyr, whereas during the last 4.6 Gyr, the mean D/H has decreased from  $2.5 \times 10^{-5}$  to  $1.5 \times 10^{-5}$ . This could seem paradoxical, but, taking into account a possible primordial infall, one could alleviate the problem of the proximity between the SBBN and present D/H ratio (Chiappini, Renda, & Matteucci 2002).

On the other hand, the accumulation of information on the high-redshift universe leads to the conclusion that there was intense activity in the past compared to the present ( $z = 0$ ).

Indeed, the cosmic star formation appears to be much higher at high  $z$  (Lanzetta et al. 2002; Hernquist & Springel 2003), and, moreover, many clues point toward the existence of an early generation of massive stars (Silk 2003; Cen 2003). In this case, the parameters governing global galactic evolution (initial mass function, star formation rate [SFR], . . .) should be reconsidered (see Scully et al. 1997; F. Daigne et al. 2004, in preparation). In this context, the local D abundance is only representative of the local interstellar medium and not of the general star formation history of our Galaxy and, a fortiori, of the whole universe. All the more so, the *Far-Ultraviolet Spectroscopic Explorer* mission has revealed a complex

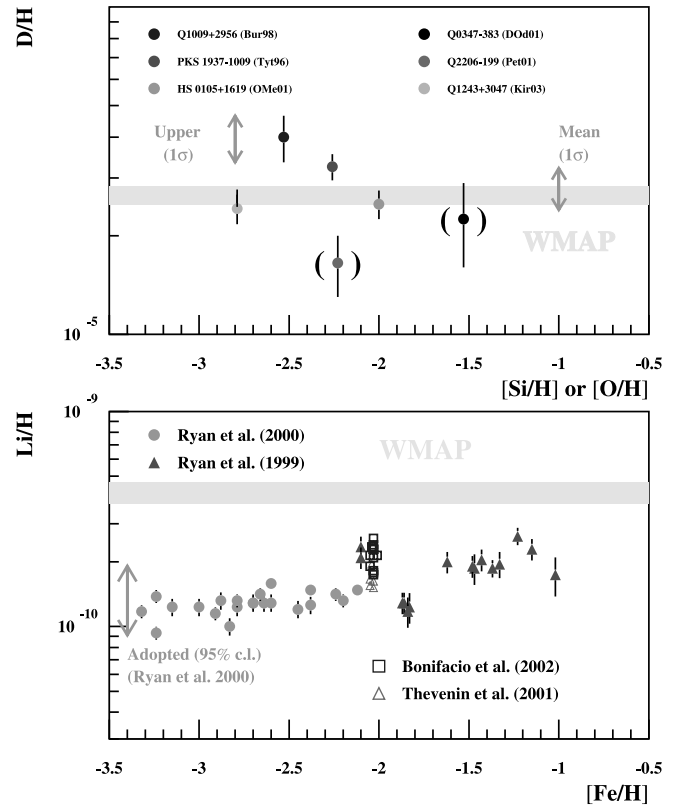


FIG. 2.—Observed abundances as a function of metallicity from objects that are expected to reflect primordial abundances. *Top*: Observed D abundances in cosmological clouds (parentheses indicate less established observations). The mean observational value (Kirkman et al. 2003) and the highest observed value used in CV02 are shown by arrows. The horizontal stripe represents the ( $1\sigma$ )  $\Omega_b h^2$  limits provided by *WMAP*+SBBN. *Bottom*: Observed  $^7\text{Li}$  abundances from Ryan et al. (1999, 2000) and extrapolated primordial abundance from Ryan et al. (2000) shown by an arrow. Li/H observations in a globular cluster at  $[\text{Fe}/\text{H}] = -2$  (Thévenin et al. 2001; Bonifacio et al. 2002) are also displayed. The horizontal stripe represents the ( $1\sigma$ )  $\Omega_b h^2$  limits provided by *WMAP*+SBBN. [See the electronic edition of the *Journal* for a color version of this figure.]

landscape for the D abundance within regions in the solar neighborhood. Indeed, although Moos et al. (2002) did not find any noticeable D variation within 100 pc (the Local Bubble), Hoopes et al. (2003) find a D/H ratio of less than  $10^{-5}$  on longer lines of sight (a few hundred parsecs). A third observed line of sight leads to an even lower D abundance,  $D/H = 0.52 \pm 0.09 \times 10^{-5}$  (Hébrard & Moos 2003). Finally, these new results show clearly that it is dangerous to take as a reference any local value of D/H without considering the systematic errors in the determination of the H column densities (Vidal-Madjar & Ferlet 2002). Starting from the primordial D/H deduced from *WMAP*+SBBN, one can predict, according to specific SFR histories versus  $z$  (which are probably highly variable from one type of galaxy to the other; see Kauffmann et al. 2003), very different present D abundances in spiral and elliptical galaxies. (F. Daigne et al. 2004, in preparation).

#### 4.3. Lithium

Contrary to deuterium, lithium presents a neat discrepancy. Indeed, our value deduced from *WMAP*+SBBN is  ${}^7\text{Li} = (4.15_{-0.45}^{+0.49}) \times 10^{-10}$ , while the most recent observations of lithium in halo stars lead to the range  $\text{Li}/\text{H} = (1.23_{-0.32}^{+0.68}) \times 10^{-10}$  (95% confidence level; Ryan et al. 2000). Hence, this observed Li/H is a factor of 3.4 lower than the *WMAP*+SBBN value. Even when considering the corresponding uncertainties, the two Li/H values differ statistically ( $\sim 3 \times 10^{-7}$  probability). This confirms the previous conclusions of ourselves (CV02) and others (CFO01; Cyburt et al. 2003) that the  $\Omega_b h^2$  range deduced from SBBN of  ${}^7\text{Li}$  is only marginally compatible with that from the CMB observations available at this time. Considering the different nuclear reaction rate analyses involved (NACRE; NB00; CFO01; DAA03), this result is robust with respect to nuclear uncertainties concerning the main SBBN reactions. It is strange that the major discrepancy affects  ${}^7\text{Li}$ , since it could a priori lead to a more reliable primordial value than deuterium because of much higher observational statistics and an easier extrapolation to primordial values. In Figure 2 (*bottom*) are shown the most recent  ${}^7\text{Li}$  observations by Ryan et al. (1999, 2000) as a function of metallicity for old halo stars together with their extrapolated primordial Li/H. The data of Thévenin et al. (2001) and Bonifacio et al. (2002) are also included. This figure emphasizes a strong incompatibility between *WMAP*+SBBN and measurements made in halo stars. This large difference could have various causes.

The first one, of observational nature, concerns systematic uncertainties on the Li abundances. As said previously, the derivation of the lithium abundance in halo stars with the high precision needed requires a fine knowledge of the physics of stellar atmospheres (effective temperature scale, population of different ionization states, non-LTE [NLTE] effects in one dimension, and further effects in three dimensions; Asplund, Carlsson, & Botnen 2003). However, the three-dimensional NLTE abundances are very similar to the one-dimensional LTE results, but nevertheless, three-dimensional models are now compulsory for extracting lithium abundances from metal-poor halo stars (see also Barklem, Belyaev, & Asplund 2003).

Second, modification of the surface abundance of Li by nuclear burning all along the stellar evolution is discussed for a long time in the literature. There is no lack of phenomena to disturb the Li abundance (rotational induced mixing, mass

loss; see Théado & Vauclair 2001; Pinsonneault et al. 2002). However, the flatness of the plateau over 3 decades in metallicity and the relatively small dispersion of data represent a real challenge to stellar modeling. New data on  ${}^6\text{Li}$  in halo stars are eagerly awaited, since they will constrain more severely the potential destruction of  ${}^7\text{Li}$  (see Vangioni-Flam et al. 1999). Finally, even taking into account the Li upper limit of the Bonifacio et al. (2002) evaluation, the inconsistency persists.

The origin of the discrepancy between the *WMAP*+SBBN Li/H calculated value and that deduced from halo star observations remains a challenging issue. Large systematic errors on the 12 main nuclear cross sections are excluded (DAA03), requiring new physics to be invoked so that large observational biases can also be excluded. Both SBBN and CMB models use the minimal number of potential parameters (even a single one for SBBN), so that their extensions can be considered. For instance, recent theories that could affect SBBN include the time variation of coupling constants (Ichikawa & Kawasaki 2002), the modification of the expansion rate during SBBN induced by quintessence (Salati 2003), modified gravity (Serna et al. 2002), and neutrino degeneracy (Orito et al. 2002). These are fundamental issues on which SBBN and CMB analyses could shed light. However, first of all, the influence of *all* nuclear reactions needs to be evaluated before any conclusion.

#### 5. NUCLEAR UNCERTAINTIES

The Monte Carlo calculations using the DAA03 rate uncertainties introduced above provide global uncertainties on yields. Here we present the effect of individual rate uncertainties for the main reactions (DAA03) but also for other reactions that have been, up until now, neglected. It is well known that the valley-shaped curve representing Li/H as a function of  $\eta$  is due to two modes of  ${}^7\text{Li}$  production. One, at low  $\eta$ , produces  ${}^7\text{Li}$  directly via  ${}^3\text{H}(\alpha, \gamma){}^7\text{Li}$ , while  ${}^7\text{Li}$  destruction comes from  ${}^7\text{Li}(p, \alpha){}^4\text{He}$ . The other one, at high  $\eta$ , leads to the formation of  ${}^7\text{Be}$  through  ${}^3\text{He}(\alpha, \gamma){}^7\text{Be}$ , while  ${}^7\text{Be}$  destruction by  ${}^7\text{Be}(n, p){}^7\text{Li}$  is inefficient because of the lower neutron abundance at high density ( ${}^7\text{Be}$  later decays to  ${}^7\text{Li}$ ). Since the *WMAP* results point toward the high- $\eta$  region, we pay particular attention to  ${}^7\text{Be}$  synthesis.

In Table 2 are given the maximum uncertainties on  ${}^4\text{He}$ , D,  ${}^3\text{He}$ , and  ${}^7\text{Li}$  isotopes arising from the rates of the 10 main nuclear reactions involved in SBBN using the results of DAA03. More precisely,  $X_{\text{high}}$  and  $X_{\text{low}}$  represent the mass fractions of a given isotope when one of the reaction rates is set to its  $+1 \sigma$  and  $-1 \sigma$  limit, respectively, and to the *maxima* of the quantities  $X_{\text{high}} - X_{\text{low}}$  for  ${}^4\text{He}$  and  $\log(X_{\text{high}}/X_{\text{low}})$  [i.e., dex] for the other isotopes. By “maximum,” we mean the maximum absolute value as  $\eta$  spans the range between  $10^{-10}$  and  $10^{-9}$ . Variations lower than 0.01 dex ( $10^{-3}$  for  $Y_p$ ) are not shown. From this table, we see that the reactions whose uncertainties most affect  ${}^7\text{Li}$  are  ${}^2\text{H}(p, \gamma){}^3\text{He}$ ,  ${}^3\text{H}(\alpha, \gamma){}^7\text{Li}$ , and  ${}^7\text{Li}(p, \alpha){}^4\text{He}$  for the low- $\eta$  region and  ${}^3\text{He}(\alpha, \gamma){}^7\text{Be}$  for the high- $\eta$  region of interest.

Since we are now interested in the precise determination of the isotopic yields, it is important to check that besides the 12 main reactions of SBBN, the remaining ones are sufficiently known and do not induce any further uncertainties. Rather than estimating the uncertainties on tens of reaction rates and calculating the corresponding uncertainties on the yields, we calculate the yield variations when the rates are scaled by

TABLE 2  
INFLUENTIAL REACTIONS AND THEIR SENSITIVITY TO NUCLEAR UNCERTAINTIES  
FOR THE PRODUCTION OF  ${}^4\text{He}$ , D,  ${}^3\text{He}$ , AND  ${}^7\text{Li}$  IN SBBN

Reactions	${}^4\text{He}$	D	${}^3\text{He}$	${}^7\text{Li}$
${}^2\text{H}(p, \gamma){}^3\text{He}$ .....	...	-0.030	0.022	0.034
${}^2\text{H}(d, n){}^3\text{He}$ .....	...	-0.009	0.007	0.011
${}^2\text{H}(d, p){}^3\text{H}$ .....	...	-0.008	-0.008	0.003
${}^3\text{H}(d, n){}^4\text{He}$ .....	...	...	-0.003	-0.004
${}^3\text{H}(\alpha, \gamma){}^7\text{Li}$ .....	...	...	...	0.038
${}^3\text{He}(d, p){}^4\text{He}$ .....	0.0022	...	-0.018	-0.017
${}^3\text{He}(n, p){}^3\text{He}$ .....	...	...	-0.006	-0.004
${}^3\text{He}(\alpha, \gamma){}^7\text{Be}$ .....	...	...	...	0.049
${}^7\text{Li}(p, \alpha){}^4\text{He}$ .....	...	...	...	-0.039
${}^7\text{Be}(n, p){}^7\text{Li}$ .....	...	...	...	-0.003

NOTE.—The values shown for  ${}^4\text{He}$  are  $(X_{\text{high}} - X_{\text{low}})_{\text{max}}$ , and the values shown for D,  ${}^3\text{He}$ , and  ${}^7\text{Li}$  are  $[\log(X_{\text{high}}/X_{\text{low}})]_{\text{max}}$ .

arbitrary factors. If the variation of a reaction rate induces a significant change in the yield, it will be the signal that this reaction should be studied in closer detail and that the rate uncertainty should be calculated. This is based on the prejudice that most of the reactions between  $A = 1$  and 12 have a negligible influence on isotope yields, and hence that they need not be known precisely. To do so, we allowed the rates of the 43 reactions between  ${}^2\text{H}(n, \gamma){}^3\text{H}$  and  ${}^{11}\text{C}(p, \gamma){}^{12}\text{N}$ , whose rate uncertainties are not documented, to vary by factors of 10, 100, and 1000 above their nominal rate and calculated the corresponding variation on the  ${}^4\text{He}$ , D,  ${}^3\text{He}$ , and  ${}^7\text{Li}$  yields. (Since the contribution of these reactions to these four isotopes is already considered negligible, it is irrelevant to consider lower rates.) In many cases, these factors may be excessive because the rates are based on the analysis of existing experimental data or on theory. However, one should note, for instance, that in the new NACRE compilation (Angulo et al. 1999), several rates differ from the previous ones (CF88) by

several orders of magnitude. This is the case, in particular, of the  ${}^{10}\text{B}(p, \alpha){}^7\text{Be}$  reaction, whose rate has drastically changed between CF88 and NACRE because of new experimental data (Angulo et al. 1993). This has led to a change of a factor of  $\approx 10$  in the SBBN  ${}^{10}\text{B}$  yield (Vangioni-Flam et al. 2000). In addition, several rates come from estimates that have not been revisited for more than 30 years and could be obsolete or wrong by unpredictable factors. This might happen, in particular, for reactions involving unstable nuclei. For instance, in another context, the  ${}^{18}\text{F}(p, \alpha)$  reaction rate remains uncertain by several orders of magnitude, even at a few  $10^8$  K (Coc et al. 2000), so as a first step, we use these arbitrary variations, in many cases excessive, to select the most influential reaction rates. In that way, we can eliminate from a more detailed study the many reactions whose influences remain negligible, even if their rate is increased by a factor as large as 1000. Then, as a second step, having drastically reduced the number of reactions, we discuss their actual nuclear uncertainties.

TABLE 3  
TEST OF YIELD SENSITIVITY TO REACTION RATE VARIATIONS: FACTORS OF 10, 100, AND 1000<sup>a</sup>

Reaction	References	${}^4\text{He}$	D	${}^3\text{He}$	${}^7\text{Li}$
${}^2\text{H}(n, \gamma){}^3\text{H}$ .....	1	0.003	...	...	...
		0.025	-0.010	...	-0.011
		0.110	-0.073	-0.048	-0.078
${}^3\text{H}(p, \gamma){}^4\text{He}$ .....	2	...	...	0.012	0.074
		0.003	-0.017	0.055	0.26
		0.018	-0.058	0.14	-0.56
${}^3\text{He}(t, np){}^4\text{He}$ .....	2	...	...	...	...
		...	...	...	-0.012
		...	0.053	-0.026	-0.092
${}^4\text{He}(\alpha, n){}^7\text{Be}$ .....	1	...	...	...	-0.056
		...	...	...	-0.36
		...	...	...	-1.1
${}^7\text{Li}(d, n)2 {}^4\text{He}$ .....	3	...	...	...	-0.10
		...	...	...	-0.44
		...	...	...	-1.1
${}^7\text{Li}(t, 2n)2 {}^4\text{He}$ .....	4	...	...	...	...
		...	...	...	...
		...	...	...	-0.055
${}^7\text{Be}(d, p)2 {}^4\text{He}$ .....	2	...	...	...	-0.047
		...	...	...	-0.34
		...	...	...	-1.0

NOTE.—The values shown for  ${}^4\text{He}$  are  $(X_{\text{high}} - X_{\text{low}})_{\text{max}}$ , and the values shown for D,  ${}^3\text{He}$ , and  ${}^7\text{Li}$  are  $[\log(X_{\text{high}}/X_{\text{low}})]_{\text{max}}$ .

<sup>a</sup> See text.

REFERENCES.—(1) Wagoner 1969; (2) CF88; (3) Boyd et al. 1993; (4) Malaney & Fowler 1989.

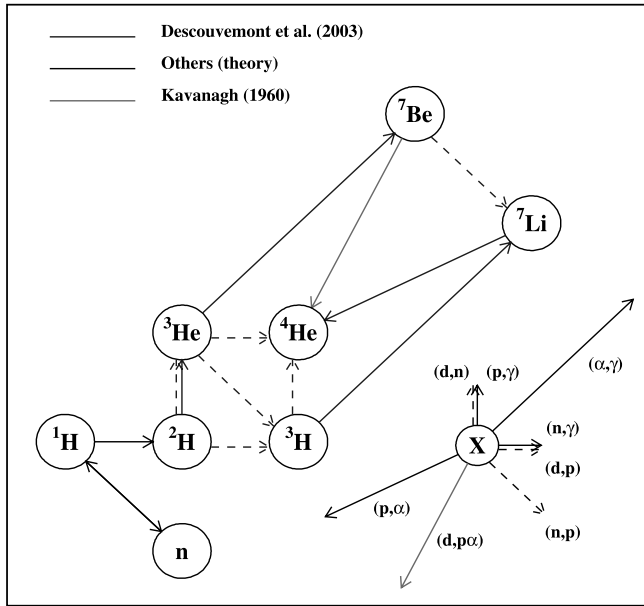


FIG. 3.—The 12 main SBBN reactions plus  ${}^7\text{Be}(d, p)2\,{}^4\text{He}$ . [See the electronic edition of the Journal for a color version of this figure.]

Table 3 lists the few reactions for which a variation of their rates by up to an arbitrary factor of 1000 induces a variation of the yields by more than 0.01 dex for  ${}^4\text{He}$ , D,  ${}^3\text{He}$ , and  ${}^7\text{Li}$ . It shows that there are only four reactions that can lead to a factor of at least 3 (0.5 dex) on  ${}^7\text{Li}$  yield when their rates are artificially increased by up to a factor of 1000:  ${}^3\text{H}(p, \gamma){}^4\text{He}$ ,  ${}^4\text{He}(\alpha, n){}^7\text{Be}$ ,  ${}^7\text{Li}(d, n)2\,{}^4\text{He}$ , and  ${}^7\text{Be}(d, p)2\,{}^4\text{He}$ . It remains to be checked whether such a huge increase in these reaction

rates is possible. As we see below, this is generally ruled out by existing data.

A factor of  $\approx 1000$  increase of the  ${}^3\text{H}(p, \gamma){}^4\text{He}$  rate would be needed to reduce the  ${}^7\text{Li}$  yield by a factor of 3. This is excluded because, since CF88, this reaction cross section has been measured precisely by Hahn, Brune, & Kavanagh (1995) and Canon et al. (2002) over the SBBN energy range. The small changes in  $S$ -factor brought by these experiments (e.g., a  $\approx 40\%$  reduction relative to CF88 at a Gamow peak energy corresponding to  $T_9 = 1$ ) rule out any possible influence in SBBN. In any case, as seen in Figure 3, this reaction could only affect the low baryonic density branch,  ${}^3\text{H}(\alpha, \gamma){}^7\text{Li}$ , and not the *WMAP* density region.

The reaction rate for  ${}^7\text{Li}(d, n)2\,{}^4\text{He}$  comes from an analysis by Boyd, Mitchell, & Meyer (1993) of  ${}^7\text{Li}$  destruction in SBBN. A factor of 100 increase could reduce the  ${}^7\text{Li}$  production by a factor of  $\approx 3$ . Even though no rate uncertainties are provided by Boyd et al., this seems quite unlikely, since their analysis is based on experimental data available in the SBBN energy range. Nevertheless, as for the previous reaction, this could only influence the direct  ${}^7\text{Li}$  formation, i.e., the low baryonic density region.

On the contrary, the  ${}^4\text{He}(\alpha, n){}^7\text{Be}$  reaction ( $Q = -18.99$  MeV) could affect  ${}^7\text{Li}$  production at high  $\eta$ , at which it is formed as  ${}^7\text{Be}$  (Fig. 3), and through  ${}^7\text{Be}$  destruction by the reverse reaction,  ${}^7\text{Be}(n, \alpha\gamma){}^4\text{He}$ . However, the rate of this latter is negligible compared to the main destruction mechanism:  ${}^7\text{Be}(n, p){}^7\text{Li}$  (Fig. 3), where an  $l = 0$  resonance dominates, while  $l = 0$  is forbidden in  ${}^7\text{Be}(n, \alpha\gamma){}^4\text{He}$  because of the symmetry of the outgoing channel.

The last reaction in Table 3,  ${}^7\text{Be}(d, p)2\,{}^4\text{He}$ , is then the most promising in view of reducing the discrepancy between SBBN,  ${}^7\text{Li}$ , and CMB observations, and  ${}^7\text{Be} + d$

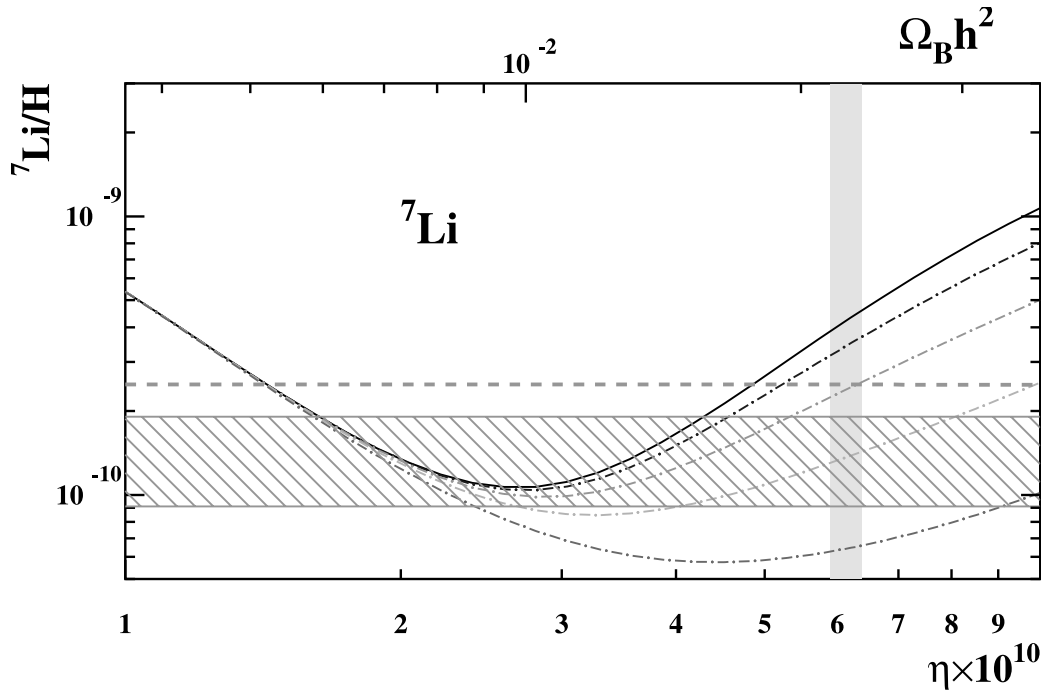


FIG. 4.—Same as Fig. 1 (bottom), but including the effect of  ${}^7\text{Be}(d, p)2\,{}^4\text{He}$  rate variations, while other reaction rates are set to their nominal values. The solid curve is the reference for which the  ${}^7\text{Be}(d, p)2\,{}^4\text{He}$  rate from CF88 is used, while the dot-dashed curves correspond to an increase of the rate by factors of 30, 100, 300, and 1000. [See the electronic edition of the Journal for a color version of this figure.]

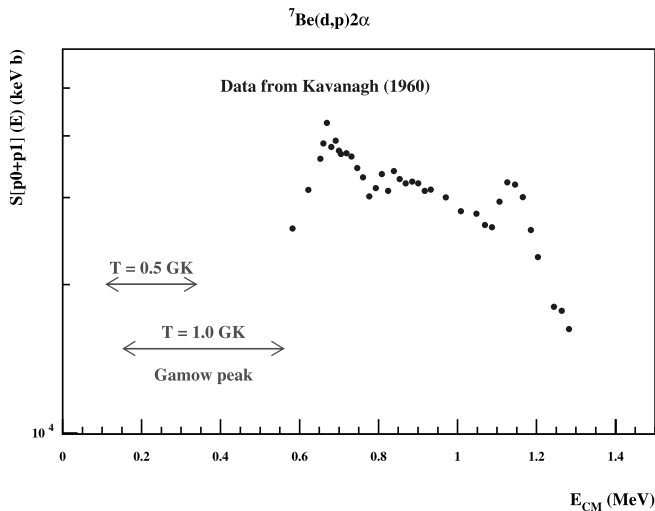


FIG. 5.—Only experimental data available for the  ${}^7\text{Be}(d, p)2\,{}^4\text{He}$  reaction from Kavanagh (1960). The displayed  $S$ -factor is calculated as in Parker (1972) from the differential cross section at  $90^\circ$  (multiplied by  $4\pi$ ), leading to the ground and first  ${}^8\text{Be}$  excited states. Note that no data are available at SBBN energies, as shown by the Gamow peaks for  $T_9 = 1$  and  $0.5$ . [See the electronic edition of the Journal for a color version of this figure.]

could be an alternative to  ${}^7\text{Be}(n, p){}^7\text{Li}$  for the destruction of  ${}^7\text{Be}$  (see Fig. 3) by compensating for the scarcity of neutrons at high  $\eta$ . Figure 4 shows the effect of an increase of the  ${}^7\text{Be}(d, p)2\,{}^4\text{He}$  reaction rate: a factor of  $\geq 100$  could alleviate the discrepancy. The rate for this reaction (CF88) can be traced to an estimate by Parker (1972), who assumed for the astrophysical  $S$ -factor a constant value of  $10^5$  keV barns. This is based on the single experimental data set available (Kavanagh 1960). To derive this  $S$ -factor, Parker used the measured differential cross section at  $90^\circ$  and assumed isotropy of the cross section. Since Kavanagh measured only the  $p_0$  and  $p_1$  protons (i.e., feeding the  ${}^8\text{Be}$  ground and first excited levels), Parker introduced an additional but arbitrary factor of 3 to take into account the possible population of higher lying levels. Indeed, a level at 11.35 MeV is also reported (Ajzenberg-Selove 1988). This factor should also include the contribution of another open channel in  ${}^7\text{Be} + d$ :  ${}^7\text{Be}(d, \alpha){}^5\text{Li}$ , for which no data exist. The experimental data

(Kavanagh 1960) are displayed in Figure 5, showing the two expected resonances at 0.7 and 1.2 MeV (Ajzenberg-Selove 1988).<sup>2</sup> A third one at 0.6 MeV is excluded because of isospin selection rules.  ${}^7\text{Li}$  and  ${}^7\text{Be}$  SBBN take place when the temperature has decreased below  $T_9 = 1$ . The Gamow peaks for  $T_9 = 1$  and  $0.5$  displayed in Figure 5 show that there are no experimental data at SBBN energies. A seductive possibility for reconciling SBBN,  ${}^7\text{Li}$ , and CMB observations would then be to get new experimental data below  $E_d = 700$  keV ( $E_{\text{cm}} \approx 0.5$  MeV) for  ${}^7\text{Be}(d, p)2\,{}^4\text{He}$  [and  ${}^7\text{Be}(d, \alpha){}^5\text{Li}$ ], leading to a sudden increase in the  $S$ -factor, as in  ${}^{10}\text{B}(p, \alpha){}^7\text{Be}$  (NACRE). This is not supported by known data, but considering the cosmological or astrophysical consequences, this is definitely an issue to be investigated. Accordingly, an experimental study of this reaction will be performed soon at Louvain la Neuve.

## 6. CONCLUSIONS

In conclusion, the recent *WMAP* experiment has to be acknowledged for making great progress, specifically concerning the evaluation of the baryon content of the universe. This leads nuclear astrophysicists to refine their calculations. We have improved SBBN calculations by taking into account a new nuclear physics analysis (DAA03) of SBBN reaction rates. The consistency between *WMAP* results and D/H data from the remote cosmological clouds in the line of sight of high-redshift quasars strengthens the deduced baryonic density. However, a significant discrepancy is observed for lithium. Nuclear effects, in particular higher  ${}^7\text{Be} + d$  reaction rates (see above), could reconcile calculations and observations. If not, new and exciting astrophysical or physical effects will have to be considered.

We warmly thank Roger Cayrel, Guillaume Hébrard, and Frédéric Thévenin for fruitful discussions. We thank also Keith Olive for his continuing useful collaboration. Finally, we thank very much Martin Lemoine for reading the manuscript. This work has been supported by PICS 1076 of INSU/CNRS.

<sup>2</sup> See the TUNL Nuclear Data Evaluation Project at <http://www.tunl.duke.edu/nucldata/fas/88AJ01.shtml>.

## REFERENCES

- Ajzenberg-Selove, F. 1988, *Nucl. Phys. A*, 490, 1  
 Angulo, C., Engstler, S., Raimann, G., Rolfs, C., Schulte, W. H., & Somorjai, E. 1993, *Z. Phys. A*, 345, 231  
 Angulo, C., et al. 1999, *Nucl. Phys. A*, 656, 3  
 Asplund, M., Carlsson, M., & Botnen, A. V. 2003, *A&A*, 399, L31  
 Bania, T. M., Rood, R. T., & Balser, D. S. 2002, *Nature*, 415, 54  
 Barker, F. C., & Kajino, T. 1991, *Australian J. Phys.*, 44, 369  
 Barklem, P. S., Belyaev, A. K., & Asplund, M. 2003, *A&A*, 409, L1  
 Bonifacio, P., et al. 2002, *A&A*, 390, 91  
 Boyd, R. N., Mitchell, C. A., & Meyer, B. S. 1993, *Phys. Rev. C*, 47, 2369  
 Brune, C. R., Hahn, K. I., Kavanagh, R. W., & Wrean, P. W. 1999, *Phys. Rev. C*, 60, 015801  
 Burles, S., Nollett, K. M., & Turner, M. S. 2001, *ApJ*, 552, L1  
 Burles, S., & Tytler, D. 1998, *ApJ*, 507, 732  
 Canon, R. S., et al. 2002, *Phys. Rev. C*, 65, 044008  
 Caughlan, G. R., & Fowler, W. A. 1988, *At. Data Nucl. Data Tables*, 40, 283  
 Cen, R. 2003, *ApJ*, 591, L5  
 Chen, J.-W., & Savage, M. J. 1999, *Phys. Rev. C*, 60, 065205  
 Chiappini, C., Renda, A., & Matteucci, F. 2002, *A&A*, 395, 789  
 Coc, A., Hernanz, M., José, J., & Thibaud, J. P. 2000, *A&A*, 357, 561  
 Coc, A., Vangioni-Flam, E., Cassé, M., & Rabiet, M. 2002, *Phys. Rev. D*, 65, 043510 (CV02)  
 Crighton, N. H. M., et al. 2003, *MNRAS*, 345, 243  
 Cyburt, R. H., Fields, B. D., & Olive, K. A. 2001, *NewA*, 6, 215 (CFO01)  
 ———. 2003, *Phys. Lett. B*, 567, 227  
 Descouvemont, P., Adahchour, A., Angulo, C., Coc, A., & Vangioni-Flam, E. 2003, *At. Data Nucl. Data Tables*, submitted (DAA03)  
 D’Odorico, D., Dessauges-Zavadsky, M., & Molaro, P. 2001, *A&A*, 368, L21  
 Fields, B. D., & Olive, K. A. 1998, *ApJ*, 506, 177  
 Hahn, K. I., Brune, C. R., & Kavanagh, R. W. 1995, *Phys. Rev. C*, 51, 1624  
 Hébrard, G., & Moos, H. W. 2003, *ApJ*, 599, 296  
 Hernquist, L., & Springel, V. 2003, *MNRAS*, 341, 1253  
 Hersant, F., Gautier, D., & Huré, J. M. 2001, *ApJ*, 554, 391  
 Hoopes, C. G., et al. 2003, *ApJ*, 586, 1094  
 Ichikawa, K., & Kawasaki, M. 2002, *Phys. Rev. D*, 65, 123511  
 Izotov, Y. I., et al. 1999, *ApJ*, 527, 757  
 Kauffmann, G., et al. 2003, *MNRAS*, 341, 33  
 Kavanagh, R. W. 1960, *Nucl. Phys.*, 18, 492  
 Kirkman, D., Tytler, D., Suzuki, N., O’Meara, J. M., & Lubin, D. 2003, *ApJS*, 149, 1  
 Lanzetta, K. M., et al. 2002, *ApJ*, 570, 492  
 Luridiana, V., et al. 2003, *ApJ*, 592, 846

- Malaney, R. A., & Fowler, W. A. 1989, *ApJ*, 345, L5  
Moos, H. W., et al. 2002, *ApJS*, 140, 3  
Nollett, K. M., & Burles, S. 2000, *Phys. Rev. D*, 61, 123505 (NB00)  
Olive, K. A. 2003, preprint (astro-ph/0301505)  
O'Meara, J. M., Tytler, D., Kirkman, D., Suzuki, N., Prochaska, J. X., Lubin, D., & Wolfe, A. M. 2001, *ApJ*, 552, 718  
Orito, M., Kajino, T., Mathews, G. J., & Wang, Y. 2002, *Phys. Rev. D*, 65, 123504  
Parker, P. D. 1972, *ApJ*, 175, 261  
Pettini, M., & Bowen, D. V. 2001, *ApJ*, 560, 41  
Pinsonneault, M. H., et al. 2002, *ApJ*, 574, 398  
Riediger, R., Petitjean, P., & Mücke, J. P. 1998, *A&A*, 329, 30  
Ryan, S. G., Norris, J., & Beers, T. C. 1999, *ApJ*, 523, 654  
Ryan, S. G., et al. 2000, *ApJ*, 530, L57  
Salati, P. 2003, *Phys. Lett. B*, 571, 121  
Scully, S., et al. 1997, *ApJ*, 476, 521  
Serna, A., et al. 2002, *Classical Quantum Gravity*, 19, 857  
Silk, J. 2003, *MNRAS*, 343, 249  
Smith, M. S., Kawano, L. H., & Malaney, R. A. 1993, *ApJS*, 85, 219  
Spergel, D. N., et al. 2003, *ApJS*, 148, 175  
Spite, F., & Spite, M. 1982, *A&A*, 115, 357  
Théado, S., & Vauclair, S. 2001, *A&A*, 375, 70  
Thévenin, F., et al. 2001, *A&A*, 373, 905  
Tytler, D., Fan, X. M., & Burles, S. 1996, *Nature*, 381, 207  
Vangioni-Flam, E., Olive, K. A., Fields, B. D., & Cassé, M. 2003, *ApJ*, 585, 611  
Vangioni-Flam, E., et al. 1999, *NewA*, 4, 245  
———. 2000, *A&A*, 360, 15  
Vidal-Madjar, A., & Ferlet, R. 2002, *ApJ*, 571, L169  
Wagoner, R. 1969, *ApJS*, 18, 247